Orientation-based FRET sensor for real-time imaging of cellular forces

Fanjie Meng and Frederick Sachs*

Center for Single Molecule Biophysics, Department of Physiology and Biophysics, The State University of New York at Buffalo, 3435 Main Street, Buffalo, NY 14214, USA

*Author for correspondence (sachs@buffalo.edu)

Accepted 26 September 2011
Journal of Cell Science 125, 743–750

doi: 10.1242/jcs.093104

Summary

Mechanical stress is an unmapped source of free energy in cells. Mapping the stress fields in a heterogeneous time-dependent environment like that found in cells requires probes that are specific for different proteins and respond to biologically relevant forces with minimal disturbance to the host system. To meet these goals, we have designed a genetically encoded stress sensor with minimal volume and high sensitivity and dynamic range. The new FRET-based sensor, called cpstFRET, is designed to be modulated by the angles between the donor and acceptor rather than the distance between them. Relative to other probes, it is physically smaller and exhibits a greater dynamic range and sensitivity and expresses well. For in vivo testing, we measured stress gradients in time and space in non-erythroid spectrin in several different cell types and found that spectrin is under constitutive stress in some cells but not in others. Stresses appear to be generated by both F-actin and tubulin. The probe revealed, for the first time, that spectrin undergoes time-dependent force modulation during cell migration. cpstFRET can be employed in vitro, in vivo and in situ, and when incorporated into biologically expressed extracellular polymers such as collagen, it can report multidimensional stress fields.

Key words: Fluorescence resonance energy transfer, Optical probe, Sensor, Mechanical stress, Spectrin, Cytoskeleton, Migration

Introduction

Physiological processes generate and are modulated by mechanical stress (Kumar and Weaver, 2009; Shyu, 2009; Wallace and McNally, 2009). Of the three free energy sources available to cells, chemical, electrical and mechanical, the latter is mostly unmapped due to a lack of probes. To begin opening this field we developed the original FRET-based stress probe called stFRET. It used an α-helix (a molecular spring) to link two GFP mutants (Meng and Sachs, 2008; Meng et al., 2008). We then developed sstFRET, which matched the mechanical compliance of common hosts by substituting a spectrin repeat for the linker (Meng and Sachs, 2011a). Grashoff and colleagues created another FRET sensor, TSMod, using a domain from spider silk as the linker (Grashoff et al., 2010). Iwai and Uyeda developed a strain sensor based on proximity imaging (PRIM) with GFP dimers (Iwai and Uyeda, 2008). These force sensors share a uniform mechanism for interpreting force: tension in the host induces strain in the linker, leading to increased distance between the donor and acceptor. The dynamic range of these sensors is limited by the nearly linear relationship between FRET efficiency and strain (Meng et al., 2008). These sensors are also relatively large, >70 kDa, and potentially perturb host function. This paper describes a new probe that uses angular orientation as the dominant variable and is physically smaller than previous probes. It expresses well in cells, making it a general tool for studying cell mechanics. We demonstrated probe efficacy by mapping stress gradients in spectrin in different cell types and demonstrated, for the first time, that stress in spectrin is modulated during cell migration.

Use of the angular dependence of FRET, as expressed in the orientation factor κ^2, can provide a wide dynamic range compared with FRET sensors modulated by distance that have a much smaller dynamic range and slope sensitivity (Meng and Sachs, 2008; Meng et al., 2008). κ^2 can vary from 0–4 depending upon the angle between donor and acceptor (Dale et al., 1979), whereas the FRET efficiency with strain is offset to the resting linker length and only linear in strain. When two GFPs are oriented side by side, κ^2 can vary from ~0 to 1 (1 when they are parallel and 0 when they are orthogonal). Thus, if the angles can be modulated by force, the probe has a wide dynamic range.

To build such a probe, we closely linked a donor–acceptor pair from a screen of circularly permutated stFRET (cpstFRET) (Baird et al., 1999). The selected monomers, cpCerulean and cpVenus, were derived from Cerulean and Venus (Nagai et al., 2002; Rizzo et al., 2004). The spectroscopic properties of the fluorophores were unaffected by the mutations. We linked them tightly together to form a FRET pair and named it cpstFRET. cpstFRET exhibited high sensitivity to stresses of 5–10 pN generated by DNA springs (Tseng et al., 2009). In solution, unstressed cpstFRET had 75% efficiency (relative to theoretical maximum of 100%), supporting the assumption of a near-parallel orientation of the chromophores. The short linker of cpstFRET reduced the probe molecular weight to 54 kDa, reducing the likelihood of adverse effects on the host.

To test the in vivo efficacy of the probe, we labeled non-erythroid spectrin, a cytoskeletal protein traditionally associated with the cell cortex. The α- and β-spectrin monomers assemble into functional dimers and these further dimerize into

higher-order oligomers. The oligomers bind to F-actin through two CH domains and crosslink to the transmembrane protein ankyrin through spectrin repeat domains 14 and 15 in the β-subunit (Baines, 2009). In the erythrocyte, erythroid cortical spectrin plays a key role in establishing the elastic properties of the cell (Discher et al., 1994). Johnson and others demonstrated that physiological shear stress might unfold spectrin with picoNewton forces (Johnson et al., 2007; Randles et al., 2007). In other cell types, notably those with a three-dimensional cytoskeleton, the stresses in spectrin have never been measured. To expand the knowledge base, we incorporated cpstFRET into the linker region of spectrin between repeat domains 10 and 11 of the α-subunit. To serve as a stress-free control, we attached cpstFRET to the C-terminal, where it is expected to dangle freely. The data show that, in general, spectrin is under resting stress and that this stress is modulated during cell migration.

To test the general applicability of the probe, we measured the stress in different cell types and found constitutive stress in bovine aortic endothelial cells (BAECs) and Madin-Darby canine kidney (MDCK) cells but not in human embryonic kidney (HEK) cells. We demonstrated in BAECs that spectrin is functionally linked to the actin–tubulin cytoskeleton because pharmacologic disruption of those components reduced stress. We found in BAECs that the constitutive stress in spectrin is not constant but varies in time and space during migration.

In this article, to avoid confusion with the traditional notation of a FRET ratio, we inverted the ratio so that increased '$_{Inv}$FRET' refers to increased tension in the host.

Results

Circularly permutated Cerulean and Venus and cpstFRET constructs

We circularly permutated Cerulean and Venus by opening the loop between two adjacent β-strands (Fig. 1A; supplementary material Fig. S1A). The new variants named cpCerulean and cpVenus had the N- and C-termini located at amino acid position 174. The original N- and C-termini were connected by a poly(G) peptide linker (Fig. 1A). cpCerulean and cpVenus retained their parental spectroscopic properties (Table 1; supplementary material Fig. S2). The quantum yield for both mutants declined slightly relative to the parents but the extinction coefficient increased, with the net result that cpCerulean is brighter than Cerulean and cpVenus is slightly dimmer than Venus. The emission and excitation peaks remained at the same wavelength. The methodology for data acquisition and processing followed the procedures we published previously (Meng and Sachs, 2011a).

cpstFRET consists of closely linked cpVenus and cpCerulean and it exhibited the robust energy transfer expected for nearly parallel dipoles (Fig. 1B–D). On the basis of a comparison of cpstFRET with the other six FRET sensors constructed to date (Fig. 1B), the barrels should be nearly parallel at rest. The probe I27stFRET has the lowest FRET (FRET ratio of 0.8) due to the long I27 linker (Rief et al., 1997). Similarly, sstFRET had a low FRET (ratio 1.0; Fig. 1C,D). For comparison, stFRETVCcp and stFRETVcpC are tandem-linked Venus and cpCerulean, and cpVenus and Cerulean, respectively (Fig. 1B; supplementary

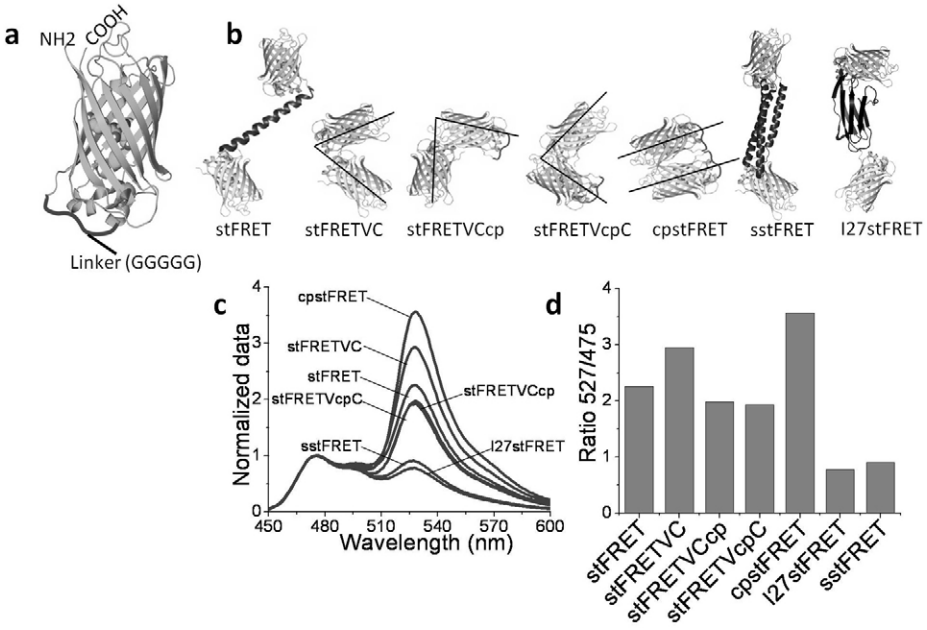

Fig. 1. FRET-based sensor constructs. (**A**) Circularly permutated donor (cpVenus) and acceptor (cpCerulean) in which the original N- and C-termini are linked by a five glycine peptide. New N- and C-termini were created at amino acid position 174. (**B**) Seven different FRET sensors that we developed. stFRET consists of Venus and Cerulean separated by a 5 nm α-helix. stFRETVC consists of Venus and Cerulean linked in tandem; substituting Cerulean by cpCerulean generates stFRETVCcp; substituting Venus by cpVenus generates stFRETVcpC, and substituting both with circularly permutated variants generates cpstFRET. sstFRET contains Venus and Cerulean separated by a spectrin repeat domain. I27stFRET contains the I27 domain from titin as the linker between Venus and Cerulean. (**C**) Spectra from purified proteins of all sensors with excitation at 433 nm and emission scan at 450 nm–600 nm. Spectra show one peak at 475 nm representing the maximum emission from Cerulean or cpCerulean, another at 528 nm representing FRET, with the maximum emission from Venus or cpVenus. All spectra were normalized to the 475 nm peak to emphasize peak shape. (**D**) Comparison of the FRET ratio (527 nm/475 nm) of seven force sensors.

Table 1. Fluorescent properties of CFP and YFP variants

Fluorescent protein*	Excitation (nm)†	Emission (nm)†	Extinction coefficient ($M^{-1}cm^{-1}$)‡	Quantum yield‡	Brightness (% of EGFP)§	p*Ka*	Photostability (wide field)
EYFP	514	527	83,400	0.61	151	6.9	60
Venus	515	528	92,200	0.57	156	6.0	15
cpVenus	515	528	158,600	0.26	122	n.d.	n.d.
ECFP	439	476	32,500	0.40	39	4.7	n.d.
Cerulean	433	475	43,000	0.62	79	4.7	36
cpCerulean	433	475	77,300	0.49	112	n.d.	n.d.

*Spectroscopic parameters determined from purified proteins (>95% homogeneity) as previously described (Meng and Sachs, 2011a; Meng and Sachs, 2011b).
†Excitation and emission wavelengths from peaks.
‡Extinction coefficients (ε) and quantum yield were determined as previously described (Meng and Sachs, 2011b).
§Brightness was calculated as the product of ε and quantum yield divided by the brightness of EGFP.
n.d., not determined.

material Fig. S1B). Despite the fact that the distance between monomers in stFRET is greater than that in stFRETVCcp or stFRETVcpC, their FRET ratio of 1.9 is less than the value of 2.2 for stFRET, which suggests that κ^2 plays a major role. Details about κ^2 applied to stFRET geometry have been published (Meng et al., 2008). The two fluorophores in stFRETVCcp and stFRETVcpC are closely fixed in distance but at unfavorable angles. We found that the closely linked pair stFRETVC (Venus and Cerulean in tandem) exhibited strong energy transfer (FRET ratio 2.9) suggesting proximity and a near parallel orientation. However, the most robust FRET occurred in cpstFRET (FRET ratio 3.8), and by analogy to the presumed parallel dimer structure of tandem GFP–cpGFP (Iwai and Uyeda, 2008), cpstFRET should also position the donor and acceptor to be nearly parallel. Force applied to the N- and C-termini of cpstFRET should disturb this nearly optimal configuration, leading to lower FRET, and thus cpstFRET can serve as a force sensor.

In vitro characterization of cpstFRET as a force sensor

To calibrate the sensitivity, we applied stress to cpstFRET in solution using a DNA spring (Wang and Zocchi, 2009; Meng and Sachs, 2011a). We covalently attached a 60mer of single-stranded DNA (ssDNA) to two locations in cpstFRET protein as previously described (Fig. 2A) to form a floppy loop. Despite the high compliance of ssDNA, simply attaching ssDNA to

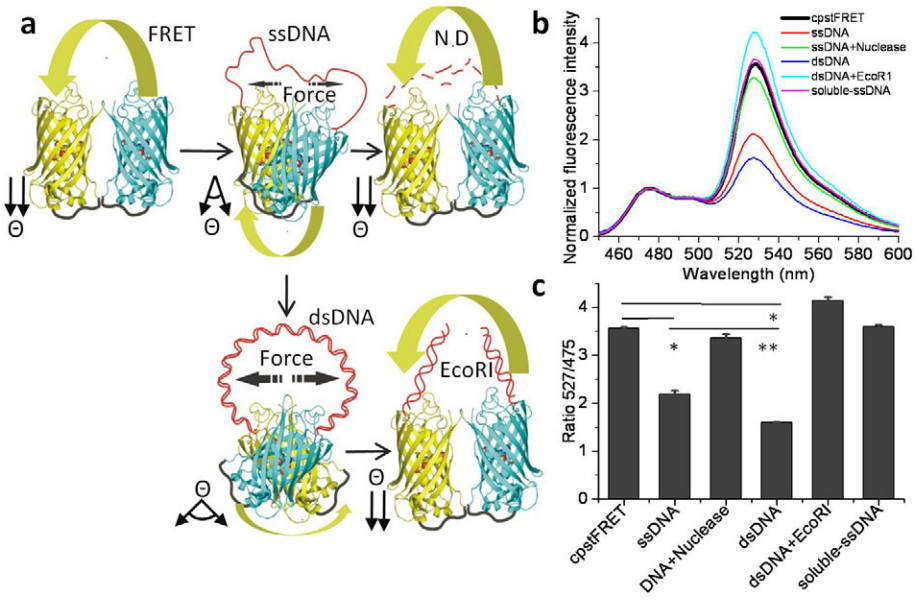

Fig. 2. Sensitivity of cpstFRET to molecular force. (**A**) ssDNA and dsDNA apply significant force to cpstFRET, leading to FRET changes. The donor is cpCerulean (cyan) and the acceptor cpVenus (yellow). Θ is the angle between donor and acceptor dipoles. At rest, a parallel orientation of donor and acceptor cpstFRET leads to robust energy transfer. Attachment of ssDNA applies <<10 pN and gently twists the monomers to an unfavorable angle causing a decrease in FRET. Complementary ssDNA anneals to the bound ssDNA and forms dsDNA that is much stiffer, further shifting the angle and decreasing FRET. Nuclease digestion (ND) breaks ssDNA and restores the control FRET with its parallel alignment. *Eco*R1 cleaves the dsDNA, releasing the force, and returns FRET to control levels. (**B**) Spectra of each of the complexes shown in A. Spectra were normalized to the cpCerulean emission 475 nm peak and scanning parameters were set as in Fig. 1. (**C**) FRET ratio of cpstFRET under DNA stretching (higher force, lower FRET ratio). Solution cpstFRET was stretched by ssDNA (ssDNA) and then digested by nuclease (DNA+Nuclease). cpstFRET was stretched by dsDNA (dsDNA) and then cleaved by *Eco*R1 (dsDNA+EcoR1). Comparison of the mixture of ssDNA and cpstFRET protein served as another control (soluble-ssDNA). Results represent mean + s.e.m. (n=3); *P<0.05, **P<0.05 (one-way ANOVA, post-hoc Tukey test).

cpstFRET led to a moderate decline in the FRET ratio from 3.6 to 2.2 (Fig. 2B,C). This suggests that the probe is sensitive to picoNewton forces. Cleavage of the bound ssDNA by nuclease restored the original (~ parallel) orientation of the donor and acceptor and fully recovered the FRET ratio. Adding complementary DNA (cDNA) to the complex created the stiffer double-stranded DNA (dsDNA) generating a force of 5–7 pN (Tseng et al., 2009). This exerted more force on the sensor and reduced the ratio to 1.5, a 60% decrease from stress-free cpstFRET. This force could be relieved with the restriction enzyme *Eco*RI that cuts through both strands of dsDNA, restoring the high FRET ratio (Fig. 2B,C). As a control for non-specific effects of DNA binding, we mixed cpstFRET protein and ssDNA in solution (soluble-ssDNA) and found no change of FRET. Thus, cpstFRET is more sensitive (60% decrease) than our previous sensor, sstFRET, which showed a 25% decrease (Meng and Sachs, 2011a). The dynamic range of FRET sensors is determined by the span from maximum to minimum FRET efficiency (E) so that cpstFRET with E=75% provides the largest dynamic range of available sensors.

We examined probe stability by exposing cpstFRET protein to denaturing concentrations of urea (supplementary material Fig. S3) and extreme pH (supplementary material Fig. S4). The monomers and cpstFRET were resistant to 8 M urea. However, pH below 6.5 decreased the fluorescence. Venus fluorescence decreased ~50% at pH 6.0 and 70% at pH 5.0 and showed a slight increase from pH 7.0 to 9.0 (supplementary material Fig. S4A). Cerulean decreased ~16% at pH 6.0 and 30% at pH 5.0 and also showed a slight increase from pH 7.0 to 9.0 (supplementary material Fig. S4B). pH also affected the FRET ratio of cpstFRET such that acidic pH 6.5 reduced FRET (emission at 527 nm) and there was almost no FRET at pH 5.0. Alkaline pH from 7.0 up to pH 10 led to a slight increase in FRET (supplementary material Fig. S4C). These results remind us that GFP-based FRET probes, in general, are sensitive to more than a single input and, ideally, the data should be obtained at different levels of acidity to check for crosstalk.

Forces in non-erythroid spectrin in living cells

We inserted cpstFRET at amino acid position 1201 in non-erythroid spectrin (Fig. 3A). The chimeric spectrin (spectrin–cpstFRET, referred to here as Spec) should not be much longer than the wild-type spectrin because the N- and C-termini of the sensor are adjacent to each other. Because both termini are located at the top of the two β-barrels, most of the sensor appears to lie perpendicular to the spectrin axis. Again, as a control, we made a spectrin tagged at the C-terminal (spectrin-C–cpstFRET, referred to here as Spec-C) where there should be no tension (Fig. 3B). We transiently expressed the chimeric spectrin constructs, free cpstFRET and a 1:1 mixture of cpCerulean and cpVenus (C+V) in BAECs (Fig. 3C,D), MDCK (Fig. 3E) and HEK cells (Fig. 3F). In cells expressing the mixture of monomers, the average distance between the two probes was large and hence exhibited negligible quenching of the donor and thus showed the highest average $_{Inv}$FRET ratio of 0.33 (donor emission intensity/acceptor emission intensity, see Materials and Methods). In Fig. 3C, $_{Inv}$FRET varied between cells due to the random amounts of cpCerulean and cpVenus DNA taken up by individual cells. The average $_{Inv}$FRET ratio from many cells approached that of a 1:1 protein mixture in solution. Cells expressing free cpstFRET showed little cell-to-cell variation and

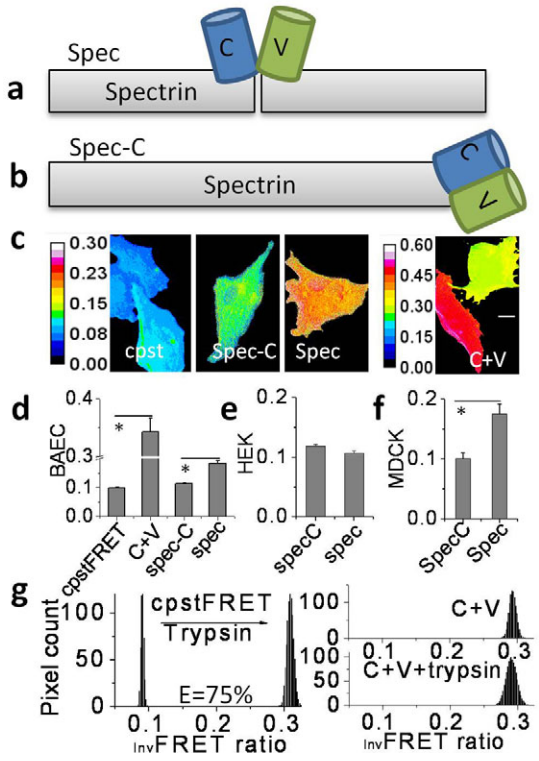

Fig. 3. Forces in non-erythroid spectrin. (**A**) Spectrin chimeric construct with cpstFRET inserted at amino acid 1201 (Spec). Donor is cpCerulean (C) and acceptor is cpVenus (V). (**B**) Spectrin tagged by cpstFRET on the C-terminal (Spec-C). (**C**) $_{Inv}$FRET images of BAECs transfected by cpstFRET (cpst), Spec, Spec-C and a 1:1 mixture of cpCerulean and cpVenus (C+V). Images were pseudo-colored using a 16-color lookup table. Scale bar: 5 µm. (**D**) $_{Inv}$FRET of BAECs expressing cpstFRET (n=20), C+V (n=15), Spec-C (n=20) and Spec (n=20). (**E**) $_{Inv}$FRET ratio of HEK cells expressing Spec-C (n=28) and Spec (n=28). (**F**) $_{Inv}$FRET of MDCK cells expressing Spec-C (n=20) and Spec (n=20). (**G**) $_{Inv}$FRET of cpstFRET and C+V in solution; pixel count distribution of $_{Inv}$FRET ratios obtained from microscopy images from donor and acceptor channels. Trypsinization eliminated FRET by cutting the linker between donor and acceptor. Based on equations developed previously (see Materials and Methods), the efficiency E reached 75%. *P<0.5 (ANOVA, post-hoc Tukey test).

a low $_{Inv}$FRET (0.10, characteristic of low stress) characteristic of robust energy transfer and a highly quenched donor signal (Fig. 3C,D). Note that in cells containing labeled spectrin, endogenous wild-type and mutant spectrin molecules might form heterotetramers, changing the observed stress. The $_{Inv}$FRET ratio seen in images is an average across all the molecules in the optical voxel. It does not represent the stress in a single molecule because there is likely to be heterogeneity in chemical composition and local stress.

In BAECs expressing labeled spectrin, $_{Inv}$FRET was 0.27, indicating the presence of significant resting stress. The host control, with cpstFRET at the C-terminal (Spec-C), sensed no force corresponding to lower $_{Inv}$FRET (0.12), similar to cells transfected with free cpstFRET (Fig. 3C,D). The algorithm to calculate $_{Inv}$FRET is insensitive to bleed-through and the inverse notation is such that a higher ratio corresponds to a larger donor signal and higher stress (Meng and Sachs, 2011a). The data shows that in BAECs spectrin bears significant constitutive stress. There was >55% increase in $_{Inv}$FRET relative to the free

sensor or to the C-terminal label, demonstrating the wide dynamic range and sensitivity of the sensor.

We measured the consistency of the microscope image analysis to the more tightly controlled fluorimeter by imaging solutions of purified proteins (Fig. 3G). The cpstFRET protein solution showed $_{Inv}$FRET of 0.10, the same as that in cells expressing free cpstFRET. After 5 minutes of trypsin cleavage of the linking region at room temperature, $_{Inv}$FRET increased to 0.30, close to that observed in cells coexpressing cpCerulean and cpVenus. Assuming force in the host can twist the transition dipoles closer to perpendicular, $_{Inv}$FRET could increase to ~0.30, a threefold change from resting to high stress, a value expected from cells. Based on our measurements of the lower and upper limits of $_{Inv}$FRET, the FRET efficiency of ~75% was the same in the image as in the spectrometer. The detailed algorithm for calculating efficiency is contained in our previous work (Meng and Sachs, 2011a). As controls for the effects of trypsin on fluorescence of the monomers, we treated a 1:1 mixture of cpCerulean and cpVenus (C+V) in solution with trypsin and found no effect, showing that the fluorophores were insensitive to trypsin (Fig. 3G, supplementary material Fig. S5B). Trypsin eliminated FRET from cpstFRET within 30 seconds by cutting the linker, and the donor signal recovered dramatically from quenching (supplementary material Fig. S5A,B).

We examined the stress in spectrin in two other cell lines, HEK and MDCK (Fig. 3E,F). HEK cells expressing Spec and Spec-C exhibited $_{Inv}$FRET of 0.11, suggesting that in these cells spectrin is stress-free. MDCK cells exhibited a higher $_{Inv}$FRET (0.18) than cells expressing Spec and a lower $_{Inv}$FRET than the control cells expressing Spec-C, indicating the presence of constitutive stress. Erythroid spectrins in red blood cells are reported to be stressed (Johnson et al., 2007). The authors used cysteine labeling and quantitative mass spectrometry of spectrin to detect unfolding induced by shear stress. They discovered that there is a significant component of unfolded spectrin at 37℃, even in resting cells, so that resting stress in erythroid spectrin probably plays an active role in determining cell shape. Further studies are clearly warranted to establish the variability of stress in spectrins and other cytoskeletal proteins in different cell types at different phases of the cell cycle, during migration, following pharmacologic perturbation, etc.

To assess the intrusive effects of probe insertion on the spectrin host we compared the histological distribution of chimeric spectrin with that of the commonly used terminal GFP tag (supplementary material Fig. S6). We found that the protein distribution and cell morphology were indistinguishable for the three constructs. We then examined the physiology by measuring the cell migration speed (supplementary material Fig. S7). Using the centroid of the cell as a marker for cell position, we found no difference between cells expressing Venus, cpstFRET, Spec or Spec-C. All cells tended to slow down with time under observation, possibly as a result of photodamage (supplementary material Fig. S7A–E). We conclude that integrating the probe into spectrin does not significantly alter cell physiology.

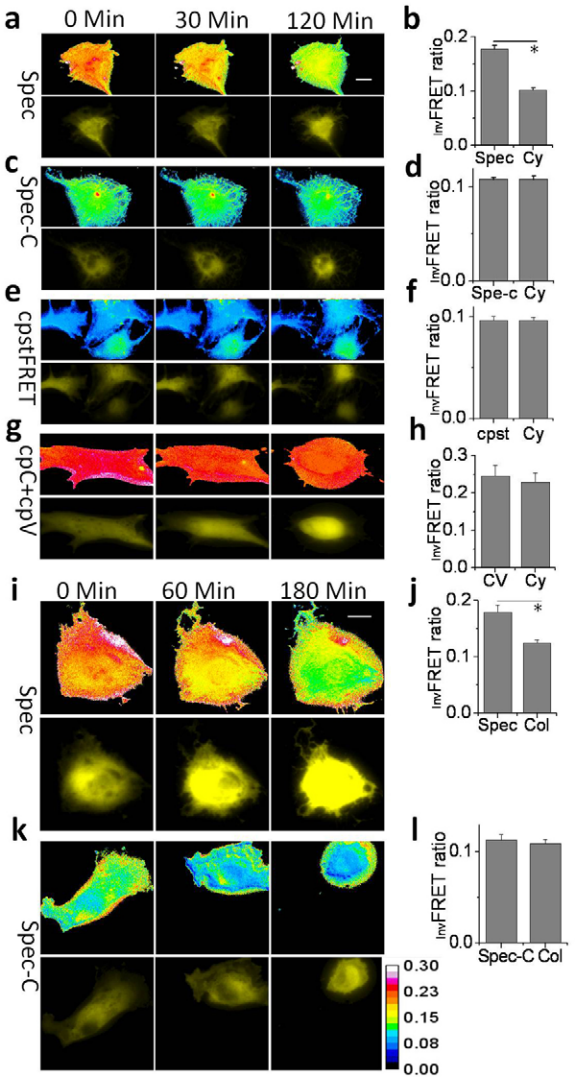

Fig. 4. Releasing molecular forces in spectrin. (**A**) Effect of treatment with cytochalasin D and latrunculin B on BAECs expressing Spec. Upper panels show $_{Inv}$FRET ratio images and lower panels show donor cpVenus in the YFP channel. (**B**) $_{Inv}$FRET of BAECs expressing Spec without treatment and after 120 minutes of treatment with 30 µM cytochalasin D and 20 µM latrunculin B (Cy). (**C**) Same as B, but for BAECs expressing Spec-C. (**D**) $_{Inv}$FRET of BAECs expressing Spec-C and the ratio after 120 minutes (P>0.1). (**E**) Same as B, but for BAECs expressing cpstFRET. (**F**) $_{Inv}$FRET of BAECs expressing cpstFRET (cpst) and the ratio after 120 minutes (P>0.1). (**G**) Same as B, but for BAECs coexpressing cpCerulean and cpVenus in a 1:1 ratio (cpC+cpV). (**H**) $_{Inv}$FRET of BAECs coexpressing cpCerulean and cpVenus (CV) and the ratio after 120 minutes (P>0.1). (**I**) Effect of treatment with 50 µM colchicine on BAECs expressing Spec. (**J**) $_{Inv}$FRET of BAECs expressing Spec and the ratio after 180 minutes of colchicine treatment (Col). (**K**) Same as I, but for BAECs expressing Spec-C. (**L**) $_{Inv}$FRET of BAECs expressing Spec-C and the ratio after 180 minutes in colchicine (P>0.1). $_{Inv}$FRET images were displayed in ImageJ using a 16-color map (bottom right). Scale bars: 10 µm. Bar graphs show means + s.e.m. (n=20); *P<0.05 (one-way ANOVA, post-hoc Tukey test).

Cytoskeleton and the forces coupling to spectrin

We examined the two major cytoskeleton components, F-actin and microtubules. We treated BAECs expressing Spec with a mixture of cytochalasin D and latrunculin B to disrupt F-actin and recorded a time series of images (Fig. 4A, supplementary material Movie 1). Within 20 minutes there was a gradual decrease in $_{Inv}$FRET, reflecting lower stress in spectrin. After 2 hours the average $_{Inv}$FRET ratio fell to the unstressed value of 0.10 (Fig. 4B, Figs 1, 3). As controls, we performed the same

studies on cells expressing Spec-C, free cpstFRET and cpCerulean plus cpVenus (Fig. 4C–H, supplementary material Movie 1). Spec-C and cpstFRET showed no change, with an $_{Inv}$FRET of ~0.10 and there were only minor changes after 2 hours. The mixture neither sensed stress nor detected changes induced by the drugs. We conclude that F-actin probably generates the constitutive force in spectrin.

Although actin fibers are known to have a direct contact to spectrin, what about the microtubules that have no such association? To answer this, we treated cells with colchicine and again recorded a time series (Fig. 4I–L; supplementary material Movie 2). During the first hour, $_{Inv}$FRET declined slowly and after 3 hours $_{Inv}$FRET decreased to 0.12, indicating reduced stress. The control, Spec-C, showed no change. Apparently, microtubules also contribute to constitutive stress in spectrin. We anticipate that other cytoskeletal proteins will show similar coupling.

The stress in cells varies during migration so we analyzed their movement over time (Fig. 5, supplementary material Movie 3). Cells expressing Spec showed large time-dependent fluctuations in $_{Inv}$FRET, indicating dynamic changes in stress. In Fig. 5A, the 'Spec' panels show two adjacent cells in the same field. At the beginning of the time series, the bottom cell showed a high $_{Inv}$FRET (~0.20, indicating high stress) and the upper one showed a lower $_{Inv}$FRET (0.12, indicating low stress). Both cells migrated to the left during the first 3 hours. $_{Inv}$FRET (stress) in the upper cell did not change whereas the bottom cell contracted and displayed a dramatic drop in $_{Inv}$FRET (supplementary material Movie 3, Fig. 5A). After 4 hours these two cells diverged. The bottom cell reversed its migration direction and started moving to the right. However, $_{Inv}$FRET and stress continued dropping to a level equal to the upper cell, which remained at low stress and maintained the same migration direction. With the upper cell serving as an internal control for the lower cell, the data showed that simple cell morphology is not a good indicator of internal stresses.

As additional controls, we monitored the migration of cells expressing Spec-C and free cpstFRET (Fig. 5A). Consistent with the absence of force, $_{Inv}$FRET remained constant throughout the 6-hour time series (Fig. 5B). We examined the data statistically for correlations between resting stress and time-dependent changes. Cells expressing Spec, with high constitutive stress, showed decreasing stress with time; cells with low constitutive stress tended to remain at constant stress over time. The average $_{Inv}$FRET of cells expressing cpstFRET and Spec-C remained low (~0.10; Fig. 5B). The data illustrate the heterogeneity of the stresses in cells and reaffirms that one cannot estimate these stresses from cell shape or traction stress on substrates.

Discussion

The design principle of cpstFRET is that the FRET depends strongly on angular orientation of the donor and acceptor. In a previous study, we deliberately changed κ^2 by varying the α-helical linker length in stFRET to produce large changes in angle with small changes in length (Meng et al., 2008). Later that year, Iwai and Uyeda reported that cpGFP and GFP joined in tandem form parallel dimers (Iwai and Uyeda, 2008). Modeling that experiment, as we reduced the length of our linker we expected a robust energy transfer but, surprisingly, neither cpCerulean–Venus nor Cerulean–cpVenus generated high FRET. However, by screening mutants we created cpstFRET that exhibited high energy transfer, implying a near-parallel orientation at rest (Fig. 1, supplementary material Fig. S1). The rigid structure of the fluorophores and our tight linker limited the variation of distance between donor and acceptor but not the angles. As we have shown, forces <10 pN can twist the structure to unfavorable orientations and cause a decrease in FRET (increase in $_{Inv}$FRET). Our improved sensitivity is demonstrated by the experiments in which the force generated with DNA springs led to larger changes with cpstFRET than with sstFRET or stFRET (Fig. 2). In an ideal case, forces in the host could rotate the angles from parallel to perpendicular so that FRET could vary from ~ 75% to 0%. cpstFRET is smaller than other probes because it has no linker domain as used in stFRET, sstFRET and TSMod (Meng et al., 2008; Grashoff et al., 2010; Meng and Sachs, 2011a). The smaller size should minimize perturbations to the host and this is supported by the data showing that cells expressing chimeric spectrin displayed normal morphology and physiological activity (supplementary material Figs S6, S7). As with most probes, the specificity of cpstFRET fluorescence is not perfect for stress alone because it displays some sensitivity to pH (supplementary material Fig. S4C). The user needs to remain aware of potential crosstalk between stimulus modalities.

We wish to emphasize that the probe does not provide an absolute measure of local stress, i.e. the absolute tension in spectrin. In a light microscope, the effective voxel size is on the order of a cubic micrometer and, within that volume, there are likely to be many labeled molecules, heterogeneity of composition (dimers of labeled, unlabeled and bilabeled hosts) and variations in local stress. The images only provide estimates

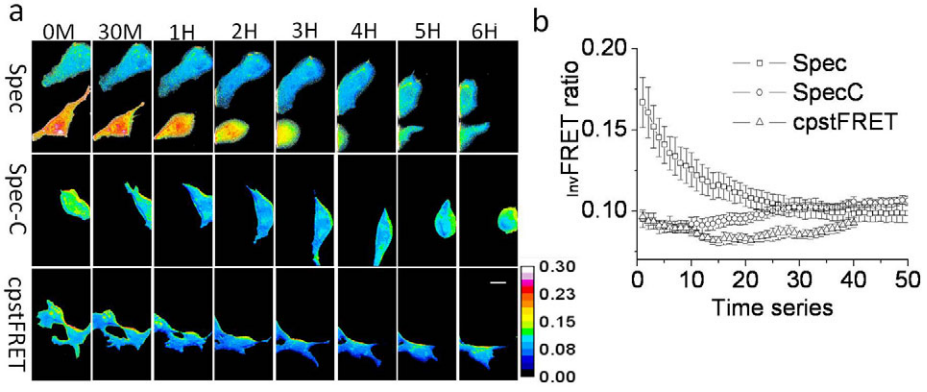

Fig. 5. Forces across spectrin network during cell migration. (**A**) $_{Inv}$FRET time series of migrating BAECs expressing Spec, Spec-C and cpstFRET. $_{Inv}$FRET images were pseudo-colored using a 16-color map (bottom right). Frames shown are spanning 0, 0.5, 1, 2, 3, 4, 5 and 6 hours. Scale bar: 20 μm. (**B**) Time series of $_{Inv}$FRET of migrating BAECs expressing Spec (n=8), Spec-C (n=8) and cpstFRET (n=6). Time series was 50 time points with 10 minute intervals. Values represent mean ± s.e.m.

of the mean stress and not the stress that one might measure in a single-molecule experiment (Oberhauser et al., 2001; Brown et al., 2007). The probes are most useful for examining gradients of stress and sources of modulation.

The constitutive stresses in spectrin appear to originate from F-actin and microtubules (Fig. 4). Even though spectrin is anchored to the cell membrane through ankyrin and transmembrane protein complexes (Baines, 2009), the bilayer itself does not appear to exert detectable force on spectrin because in HEK cells spectrin was unstressed. The variation of constitutive stress (Fig. 3E) shows that generalizing between cell types is unwise. The cytoskeleton in HEK cells and BAECs are morphologically different. Decorated by labeled α-actinin, HEK cells have fine actin fibers although BAECs have robust fibers (Meng and Sachs, 2011a). In migrating BAECs, the mean stress in spectrin decreased with time to a basal constitutive level. However, in the same culture dish there were cells exhibiting low stress, and these remained at low stress over time except for a few cells that showed increased stress after ~6 hours (supplementary material Movie 4). This heterogeneity emphasizes that we are still far from understanding the basics of cell biology because the mechanical changes were not obviously correlated with easily observable changes in cell morphology, and fixed tissue no longer has in vivo mechanical properties. Some of the variability of results in many different types of experiments might correlate with variable stresses correlated with uncontrolled culture conditions, passage number, serum or cell hereditary. We know that stresses in the cell cortex of endothelial and epithelial cells are readily modified by fluid shear stress and that these forces are probably a major factor affecting differentiation (Johnson et al., 2007; Weinbaum et al., 2010). Our data show that mechanical stress in cells should not be treated as a static variable. Mechanical signal transmission has been demonstrated to occur over long distances at the speed of nerve conduction (Na et al., 2008).

cpstFRET is a reliable and sensitive probe for studying intra- or extracellular fibrous proteins (Meng and Sachs, 2011b; Meng et al., 2011) and can be utilized with acute transfection or probably in transgenic animals. Applicable to tissue engineering, labeled matrix proteins such as collagen produced by transgenic animals could be used to create three-dimensional matrices that can report the distribution of local stress in real time.

Materials and Methods

Gene construction and protein purification

pEYFP-C1 Venus and pECFP-C1 Cerulean plasmids were generous gifts from David W. Piston, Vanderbilt University, Nashville, TN. Based on Venus and Cerulean, we constructed circularly permutated cpVenus and cpCerulean. For cpVenus, we first subcloned the gene fragments of 175Gly–239Lys from Venus into pET-52b (+) vector (Novagen, Gibbstown, NJ) by primers 5′-GGGTACCAGGATCCATGGGCGGCGTGCAGC-3′ with *Bam*HI and 5′-GAACAGCTCCTCGCCCTTGCTCACCCCGCCACCGCCGCCGAATTCCTTGTAC-3′ with *Eco*RI. Then we subcloned the gene fragments of 1Met–174Asp and connected them to the C-terminal of the first fragment (supplementary material Fig. S1). Five glycines were added between them to give flexibility. Primers were: 5′-GTACAAGGAATTCGGCGGCGGTGGCGGGGTGAGCAAGGGCGAGGAGCTGTTC-3′ with *Eco*RI and 5′-CCAGAGCGAGCTCGTCCTCGATGTTGTGGCGGATC-3′ with *Sac*I. We generated cpCerulean similarly except that a different primer was used for fragment 175Gly–239Lys, which was 5′-GGTACCAGGATCCATGGGCAGCGTGCAGC-3′ with *Bam*HI. For eukaryotic cell expression, we subcoloned cpVenus and cpCerulean into pEGFP vector with EGFP removed beforehand. Primers used were: sense 5′-CAGATCCGCTAGCATGGGCAGCGTGCAGCTCGC-3′ with *Nhe*1 for cpCerulean, and 5′-CAGATCCGCTAGCATGGGCGGCGTGCAGCTCG-3′ with *Nhe*I for cpVenus; anti-sense 5′-CCCGCGGTACCTTAGTCCTCGATGTTGTGGCGGATC-3′ for both constructs. pET-cpstFRET was created by connecting cpVenus to the C-terminal of cpCerulean in pET-52b(+) vector; primers used were: 5′-GGCGGCAGATCTATGGGCAGCGTGCAGCTCGCC-3′ with *Bgl*II and 5′-CCAGAGCGAGCTCGTCCTCGATGTTGTGGCGG-3′ with *Sac*I. Fore eukaryotic cell expression of cpstFRET, we subcloned it into pEGFP vector by primers 5′-CAGATCCGCTAGCCAGGGACCCGGGGTACCAGGATCC-3′ with *Nhe*I and 5′-GATCCCGGGCCCTTTAACTACCGCGTGGCAC-3′ with *Apa*I.

To create chimeric gene constructs of α-spectrin, we subcloned the gene encoding spectrin into pEGFP-C1 vector from which the EGFP gene was removed beforehand. The primers and restriction enzyme sites introduced into PCR products for subcloning spectrin were: sense, 5′-CTAGCGCTACCGGTATGGACCCAAGTGGGGTCAAAGTGC-3′ with *Age*I and anti-sense, 5′-CGGGCCCGCGGTACCGTTCACGAAAAGCGAGCGGGTGAAC-3′ with *Sac*II. cpstFRET was inserted into spectrin at amino acid position 1200, which located in the linker domain between the 10th and 11th spectrin repeat domains by restriction sites *Sal*I and *Not*I. The restriction enzyme sites were introduced into the host proteins by a site-directed mutagenesis kit from Stratagene (La Jolla, CA) with the host protein amino acid unchanged. We also tagged spectrin with cpstFRET or EGFP on the C-terminal as negative controls. Spectrin-EGFP can show the distribution of spectrins in cells. All construct sequences were confirmed by DNA sequencing at Roswell-Park Cancer Institute (Buffalo, NY). Protein purification followed protocols previously described (Meng et al., 2008).

Protein-DNA complex synthesis and in vitro DNA stretching

As described previously (Meng and Sachs, 2011a), a 60mer DNA, [AminoC6]GAGTGTGGAGCCTAGACCGTGAATTCCTGGCAGTGGTGCGACCGACGTGGAGCCTCCCT[AmC7Q], and the complementary strand were purchased from Operon (Huntsville, AL). The oligo has an amino modification on both ends and an *Eco*R1 cutting site in the middle. The sequence was selected on the basis of a previously published study (Wang and Zocchi, 2009). The DNA–crosslinker construct was then incubated with 1.5 nmol of purified cptFRET protein in conjugation buffer, with a total volume of 50 µl. Both donor and acceptor in cptFRET have two free sulfhydryls at Cys48 and Cys70. The 70 position is concealed inside the β-barrel and inaccessible, and the 48 position is only partially exposed. To speed the reaction of the maleimides of the DNA–crosslinker to sulfhydryls at position 48, we incubated the mixture at 37℃ for 30 minutes. Because DNA does not interfere with FRET measurements, no further purification was necessary. To further stretch cpstFRET, 15 nmol of cDNA was added to the protein–ssDNA complex. The solution was left at room temperature overnight to complete the annealing.

Cell imaging and $_{Inv}$FRET ratio calculation

As described in our previous publication (Meng and Sachs, 2011a), imaging was performed on an inverted Zeiss Axio Observer A1 equipped with an Andor Ixon DV897 back-illuminated cooled CCD camera. The images at the donor emission and acceptor emission were recorded through a Dual View (Photometrics) splitter with double band excitation filters. A LED light engine from Lumencor (Lumencor, San Francisco, CA) was used for excitation at wavelengths of 433 nm for the donor and 515 nm for acceptor. The light engine used electronic shutters to switch excitation wavelengths so there was no mechanical movement over the time series.

We calculated the $_{Inv}$FRET ratio using the relationship:

$$InvFRET\ ratio = I_d/I_a.$$

where I_a is the acceptor emission intensity with acceptor excitation and I_d is the donor emission intensity with donor excitation. The $_{Inv}$FRET ratio denotes the inverted FRET ratio and positively correlates to mechanical force. The acceptor intensity scales with protein concentration and the donor signal scales with both protein concentration and quenching due to FRET. The FRET ratio directly correlated to stress: high stress, low FRET because of less quenching and thus a higher signal from the donor. We derived the FRET efficiency E from the FRET ratio as done for sstFRET (Meng and Sachs, 2011a) yielding E=75%.

For time series image acquisition and processing, we used NIH ImageJ with Micromanager software that controlled a Lumencor illuminator, Zeiss Axio Observer A1 and Ludl motorized stage. The 433 nm and 515 nm excitation power was set at 25% maximum with an exposure time of 100 milliseconds for each time point. We used 5 or 10 minute intervals between frames of the time series. The experimental span was 250 or 500 minutes.

Spectrometry and FRET ratio calculation

We used a fluorescence spectrometer (Aminco–Bowman series 2) to measure the fluorescence of purified proteins in solution. All purified proteins were exchanged into 10 mM Tris-HCl buffer before further processing. The measurements were performed at room temperature with 200 µl of 1 µM protein. The spectrometer settings were: 4 nm bandpass, 1 nm step size, and 450–600 nm emission scan

range with excitation at 433 nm. We have used the FRET ratio as the energy transfer index: FRET ratio = I_{527nm}/I_{475nm} where I_{527nm} is the acceptor emission signal (FRET) of cpstFRET and $I_{475\ nm}$ is the donor emission signal.

Cell culture, transfection and protein expressing

BAECs, HEK cells and MDCK cells were cultured in Dulbecco's modified Eagle's medium (Gibco, Invitrogen, Carlsbad, CA) supplemented with 10% fetal bovine serum and antibiotics. Cells were spread on coverslips and allowed to grow for 24 hours. Fugene 6 (Roche, Indianapolis, IN) was used to deliver 2.0 μg per coverslip of plasmid DNA to the cells. The cells were studied 24–36 hours following transfection.

Acknowledgements

We thank David Piston (Vanderbilt University) for providing the mVenus and mCerulean vectors, Thomas Suchyna for thoughtful discussion, Phil Gottlieb for advice on the chemistry, Yuexiu Wang for preparing DNA and cells, and Mary Teeling for cell culture.

Funding

This work was supported by grants from the National Institutes of Health (R01HL054487) and The Children's Guild of Buffalo to F.S. Deposited in PMC for release after 12 months.

Supplementary material available online at
http://jcs.biologists.org/lookup/suppl/doi:10.1242/jcs.093104/-/DC1

References

Baines, A. J. (2009). Evolution of spectrin function in cytoskeletal and membrane networks. *Biochem. Soc. Trans.* **37**, 796-803.

Baird, G. S., Zacharias, D. A. and Tsien, R. Y. (1999). Circular permutation and receptor insertion within green fluorescent proteins. *Proc. Natl. Acad. Sci. USA* **96**, 11241-11246.

Brown, A. E. X., Litvinov, R. I., Discher, D. E. and Weisel, J. W. (2007). Forced unfolding of coiled-coils in fibrinogen by single-molecule AFM. *Biophys. J.* **92**, L39-L41.

Dale, R. E., Eisinger, J. and Blumberg, W. E. (1979). The orientational freedom of molecular probes. The orientation factor in intramolecular energy transfer. *Biophys. J.* **26**, 161-193.

Discher, D. E., Mohandas, N. and Evans, E. A. (1994). Molecular maps of red cell deformation: hidden elasticity and in situ connectivity. *Science* **266**, 1032-1035.

Grashoff, C., Hoffman, B. D., Brenner, M. D., Zhou, R., Parsons, M., Yang, M. T., McLean, M. A., Sligar, S. G., Chen, C. S., Ha, T. et al. (2010). Measuring mechanical tension across vinculin reveals regulation of focal adhesion dynamics. *Nature* **466**, 263-266.

Iwai, S. and Uyeda, T. Q. (2008). Visualizing myosin-actin interaction with a genetically-encoded fluorescent strain sensor. *Proc. Natl. Acad. Sci. USA* **105**, 16882-16887.

Johnson, C. P., Tang, H. Y., Carag, C., Speicher, D. W. and Discher, D. E. (2007). Forced unfolding of proteins within cells. *Science* **317**, 663-666.

Kumar, S. and Weaver, V. M. (2009). Mechanics, malignancy, and metastasis: the force journey of a tumor cell. *Cancer Metastasis Rev.* **28**, 113-127.

Meng, F. and Sachs, F. (2008). stFRET, a novel tool to study molecular force in living cells and animals. *Proquest* **Dissertation 1757060081**, 143.

Meng, F. and Sachs, F. (2011a). Visualizing dynamic cytoplasmic forces with a compliance-matched FRET sensor. *J. Cell Sci.* **124**, 261-269.

Meng, F. and Sachs, F. (2011b). Measuring strain of structural proteins in vivo in real time. In *Cardiac Mechano-Electric Coupling and Arrhythmia: From Pipette to Patient* (ed. P. Kohl, F. Sachs and M. R. Franz). Oxford: Oxford University Press.

Meng, F., Suchyna, T. M. and Sachs, F. (2008). A fluorescence energy transfer-based mechanical stress sensor for specific proteins in situ. *FEBS J.* **275**, 3072-3087.

Meng, F., Suchyna, T., Lasalovitch, E., Gronostajski, R. M. and Sachs, F. (2011). Real time FRET based detection of mechanical stress in cytoskeletal proteins. *Cell. Mol. Bioeng.* **4**, 148-159.

Na, S., Collin, O., Chowdhury, F., Tay, B., Ouyang, M. X., Wang, Y. X. and Wang, N. (2008). Rapid signal transduction in living cells is a unique feature of mechanotransduction. *Proc. Natl. Acad. Sci. USA* **105**, 6626-6631.

Nagai, T., Ibata, K., Park, E. S., Kubota, M., Mikoshiba, K. and Miyawaki, A. (2002). A variant of yellow fluorescent protein with fast and efficient maturation for cell-biological applications. *Nat. Biotechnol.* **20**, 87-90.

Oberhauser, A. F., Hansma, P. K., Carrion-Vazquez, M. and Fernandez, J. M. (2001). Stepwise unfolding of titin under force-clamp atomic force microscopy. *Proc. Natl. Acad. Sci. USA* **98**, 468-472.

Randles, L. G., Rounsevell, R. W. and Clarke, J. (2007). Spectrin domains lose cooperativity in forced unfolding. *Biophys. J.* **92**, 571-577.

Rief, M., Gautel, M., Oesterhelt, F., Fernandez, J. M. and Gaub, H. E. (1997). Reversible unfolding of individual titin immunoglobulin domains by AFM. *Science* **276**, 1109-1112.

Rizzo, M. A., Springer, G. H., Granada, B. and Piston, D. W. (2004). An improved cyan fluorescent protein variant useful for FRET. *Nat. Biotechnol.* **22**, 445-449.

Shyu, K. G. (2009). Cellular and molecular effects of mechanical stretch on vascular cells and cardiac myocytes. *Clin. Sci. (Lond.)* **116**, 377-389.

Tseng, C.-Y., Wang, A., Zocchi, G., Rolih, B. and Levine, A. J. (2009). Elastic energy of protein-DNA chimeras. *Phys. Rev. E Stat. Nonlin. Soft Matter Phys.* **80**, 061912.

Wallace, G. Q. and McNally, E. M. (2009). Mechanisms of muscle degeneration, regeneration, and repair in the muscular dystrophies. *Annu. Rev. Physiol.* **71**, 37-57.

Wang, A. and Zocchi, G. (2009). Elastic energy driven polymerization. *Biophys. J.* **96**, 2344-2352.

Weinbaum, S., Duan, Y., Satlin, L. M., Wang, T. and Weinstein, A. M. (2010). Mechanotransduction in the renal tubule. *Am. J. Physiol. Renal Physiol.* **299**, F1220-F1236.

Supplementary figure 1

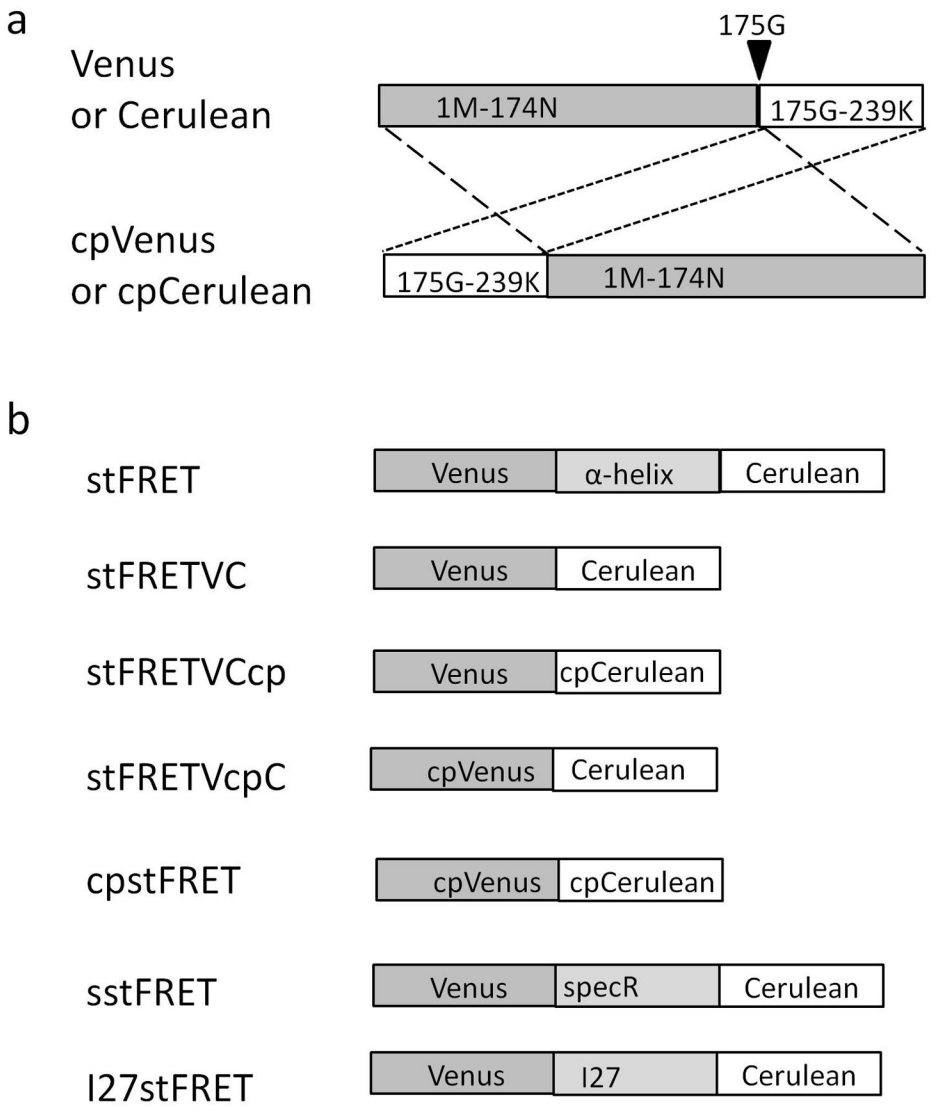

Schematic diagrams of the chimeric gene s. a, Generation of cpVenus and cpCerulean from Venus and Cerulean, dashed lines show the shuffling of the gene fragments. Arrow head indicates the circularly permutation position at glycine 175 (175G). b, All FRET force sensor constructs. SpecR is the spectrin repeat domain. I 27 is the I27 domain from titin.

Supplementary figure 2

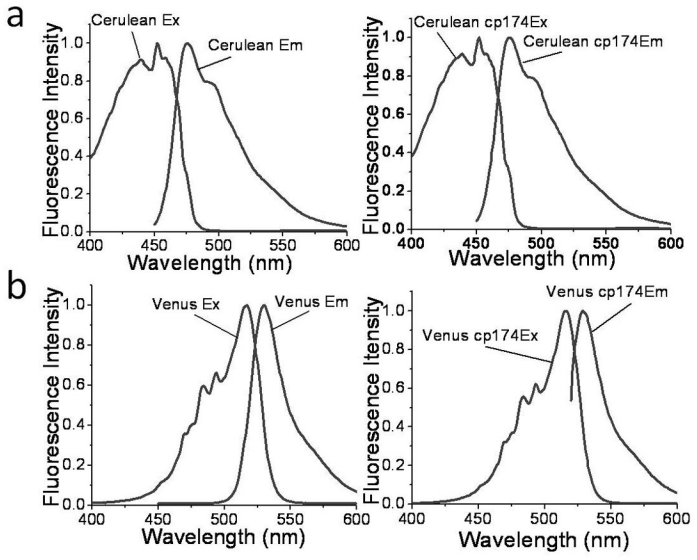

Comparison of emission and excitation spectra of cpVenus and cpCerulean to Venus and Cerulean. a, left panel, excitation and emission spectra of Cerulean, right panel, excitation and emission spectra of cpCerulean. **b**, left panel, excitation and emission spectra of Venus, right panel, cpVenus. cp174 denotes the circularly permutation sites of amino acid 174 N. The permutated constructs retained their parental proteins fluorescence characteristics.

Supplementary figure 3

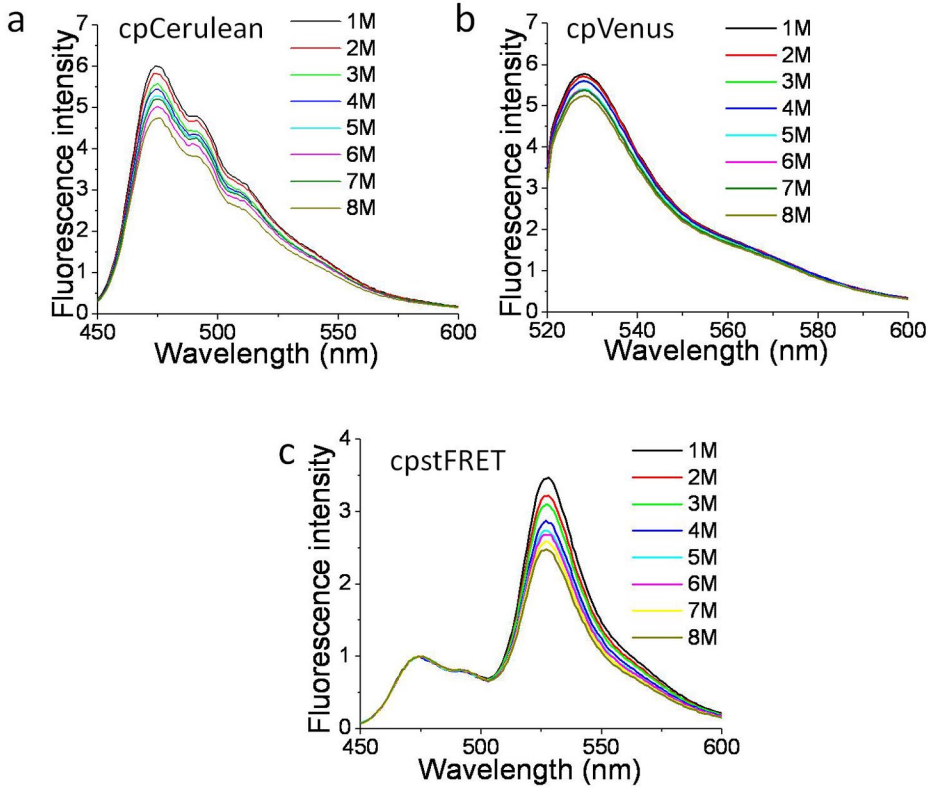

cpCerulean, cpVenus and cpstFRET are insensitive to denaturant urea. a, spectra of purified cpCerulean in 1 to 8 M urea, excitation, 433 nm, emission scan 450-600 nm. **b**, spectra of purified cpVenus in 1 to 8 M urea, excitation, 515 nm, emission scan, 520-600 nm. **c**, spectra of purified cpstFRET in 1 to 8 M urea, excitation, 433 nm, emission scan, 450-600 nm. Spectra were normalized to donor cpCerulean emission at 475 nm. Urea had minimum effect on the monomers and only slightly reduced FRET from cpstFREt (emission at 572 nm).

Supplementary figure 4

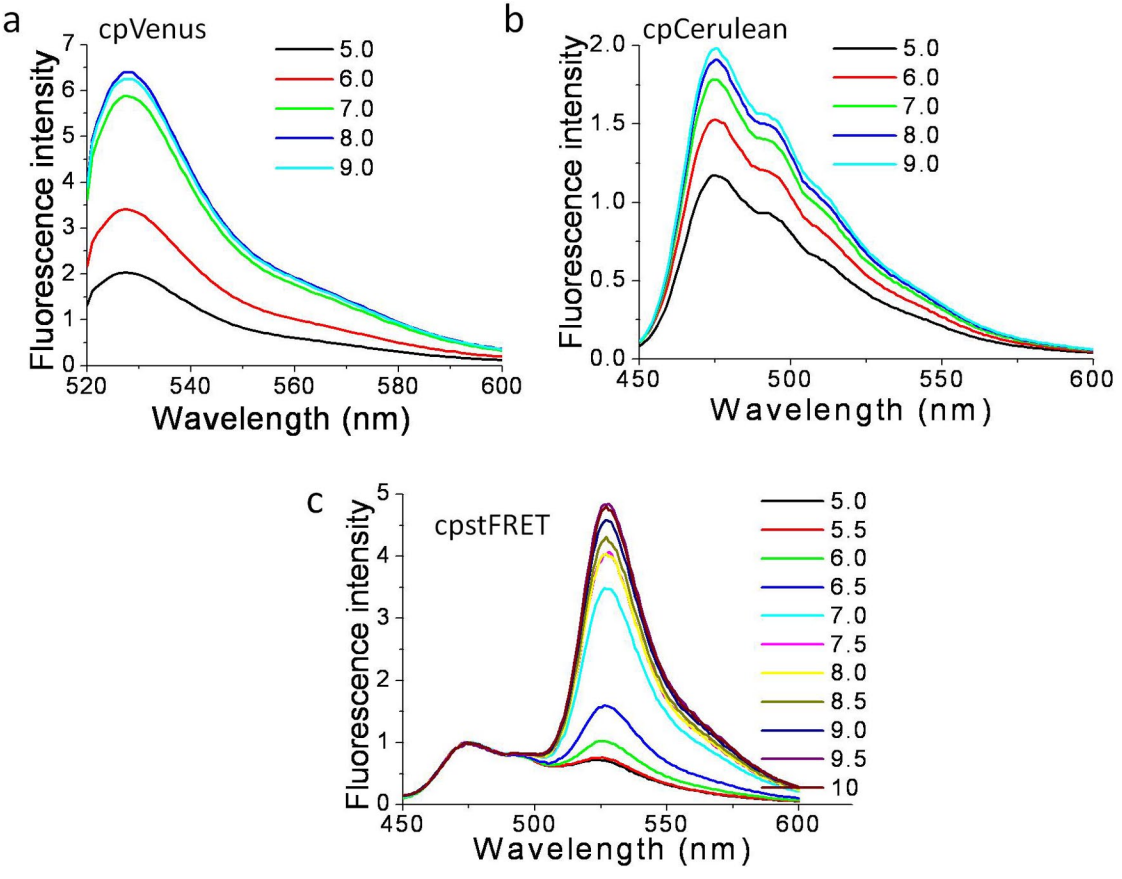

cpCerulean, cpVenus and cpstFRET are sensitive to acidic pH but not alkaline pH. a, emission spectra of purified cpVenus exposed to pH 5 to 9. **b,** spectra of purified cpCerulean exposed to pH 5 to 9. **c**, spectra of purified cpstFRET exposed to pH 5 to 10. Data acquired and processed as in supplementary figure 3. The permutated monomers and cpstFRET were highly vulnerable to acidic pH, pH < 6 led to significant fluorescence and FRET loss . Alkaline pH up to 10 slightly enhanced the FRET of cpstFRET and the fluorescence of monomers.

Supplementary figure 5

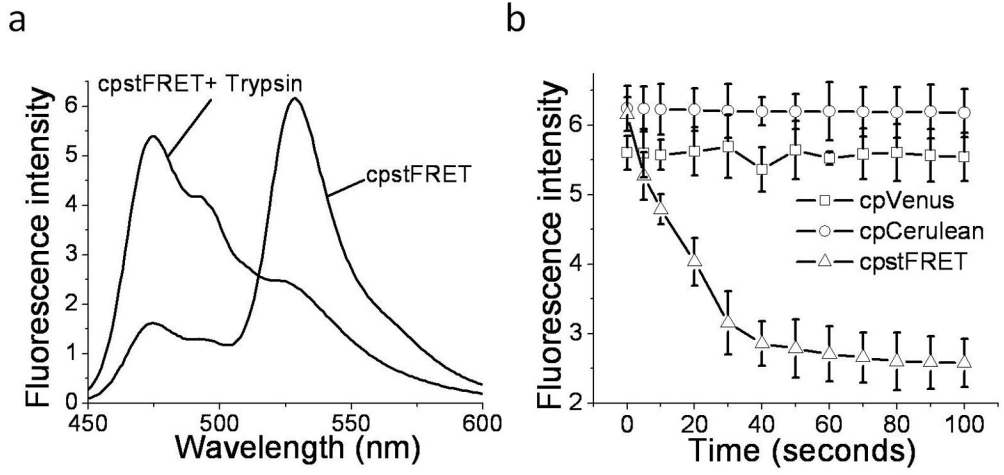

Trypsin cleaved the linker and reduced FRET in cpstFRET. **a,** spectra of cpstFRET (200 nM) and cpstFRET (200 nM) + 1 unit Trypsin at room temperature for 1 minute digestion. Excitation, 433 nm, emission scan, 450-600 nm. **b,** Time series of Trypsin digestion of cpVenus (square), cpCerulean (circle) and cpstFRET (triangle). The time series were plotted by using values of emission peaks versus time, for cpVenus the peak emission was at 527 nm, for cpCeruelan, 475 nm, for cpstFRET, peak emission was at 527 nm (FRET signal, emission from cpVenus). The excitation parameters were set as in previous figures. FRET signal diminished rapidly within 20 seconds of trypsin digestion, showing increased donor emission at 475 nm and decreased acceptor emission at 527 nm. However, the monomers were robust and remained stable fluorescence during the entire time series.

Supplementary figure 6

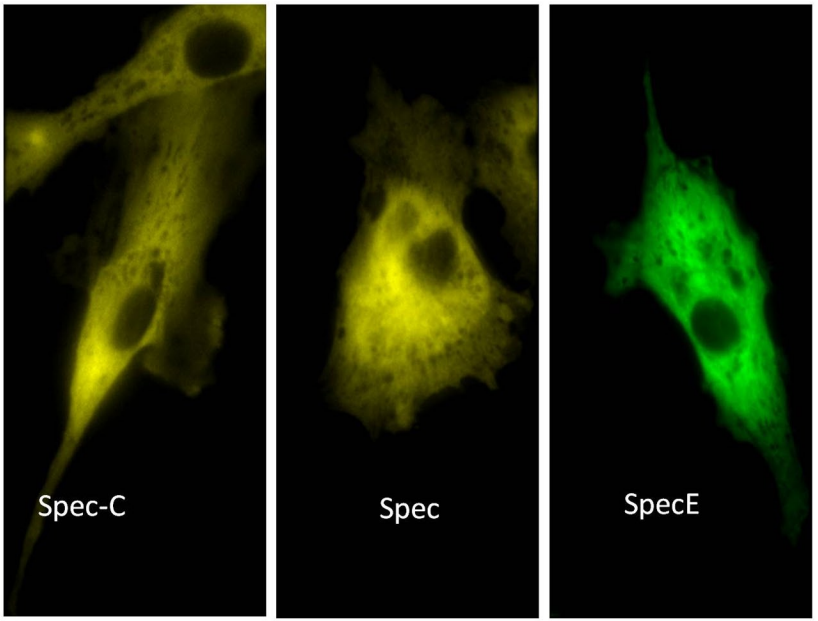

Protein distribution of tagged spectrins. Spectrin tagged by cpstFRET at C terminal (Spec-C), spectrin hosting cpstFRET in the middle (amino acid position 1201) (Spec), spectrin tagged by EGFP at C terminal (SpecE). None erythroid spectrin distributes in cortical cytoskeleton in all three cell lines, no apparent fibers or accumulations can be seen in any of the three constructs.

Supplementary figure 7

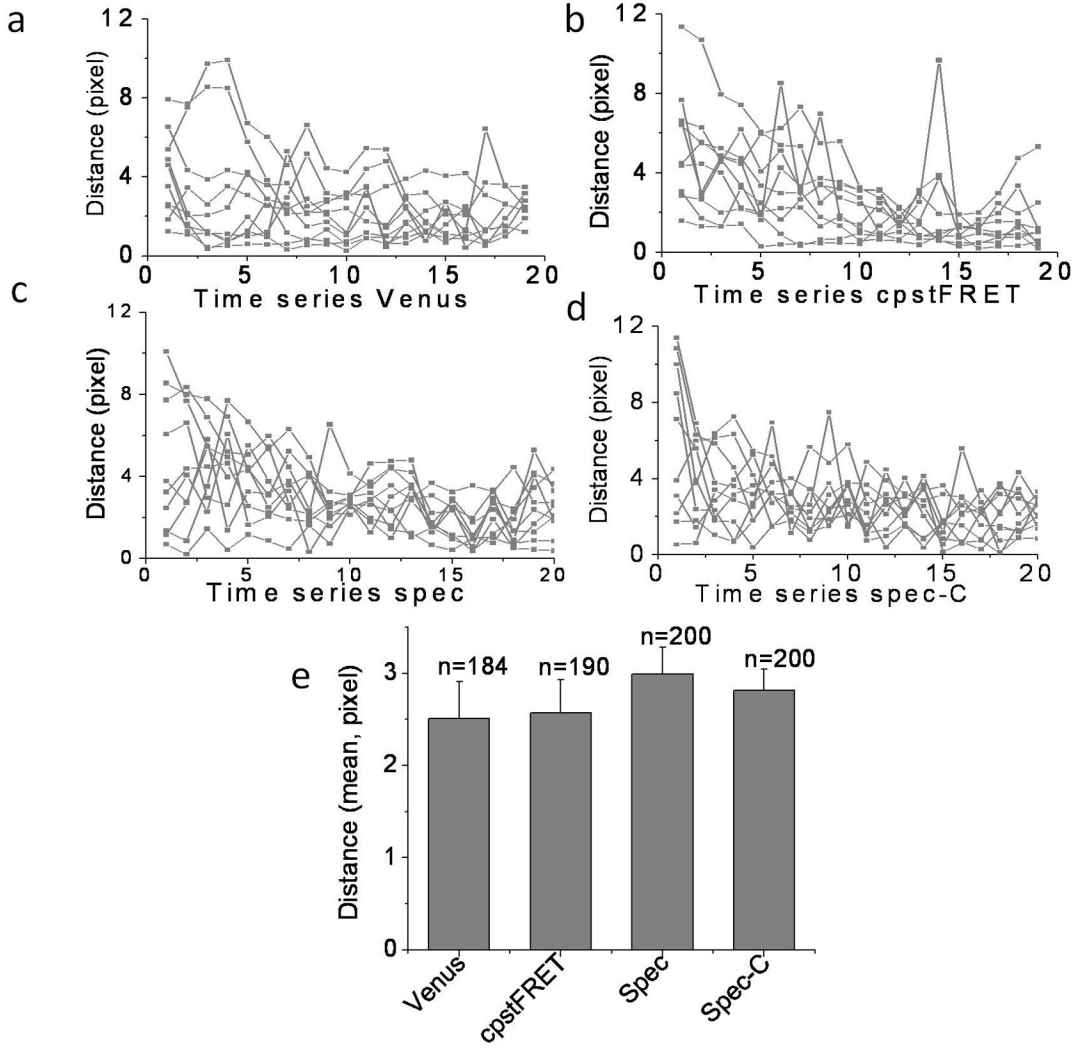

Transient expression of chimeric proteins in cells showed no adverse influences on cell migration speed. a, Plots of migration distances of centroid versus time points of YFP (Venus) expressing BAECs (n=9) . The distances during each time lapse interval were calculated by square root of ($X_{(N+1)}$-X_N)^2+($Y_{(N+1)}$-Y_N)^2, X and Y are the coordinates of the center of mass of individual cells, N is the Nth frame of the time series. The time series interval was set as 20 frames, 5 min interval. **b**, Plots of cpstFRET BAECs (n=8). **c**, Plots of Spec BAECs (n=10). **d**, Plots of Spec-C BAECs (n=10). **e**, Average migration distances of centroids of four cell lines during all 5 min intervals (ANOVA, post-hoc Turkey test, P>0.5). All error bars are SEM.